AJNR

Abnormal Brain Diffusivity in Patients with Neuropsychiatric Systemic Lupus Erythematosus

Gerlof P. Th. Bosma, Tom W. J. Huizinga, Simon P. Mooijaart and Mark A. van Buchem

AJNR Am J Neuroradiol 2003, 24 (5) 850-854
http://www.ajnr.org/content/24/5/850

AJNR Am J Neuroradiol 24:850–854, May 2003

Abnormal Brain Diffusivity in Patients with Neuropsychiatric Systemic Lupus Erythematosus

Gerlof P. Th. Bosma, Tom W. J. Huizinga, Simon P. Mooijaart, and Mark A. van Buchem

BACKGROUND AND PURPOSE: **Neuroimaging techniques have increased our knowledge of the pathogenesis of neuropsychiatric systemic lupus erythematosus (NPSLE) and have been useful in supporting the diagnosis. Nevertheless, new imaging techniques are needed to unravel the exact pathogenesis and to provide diagnostic criteria for NPSLE. In this preliminary study, we investigated whether diffusion-weighted imaging (DWI) can depict cerebral abnormalities in patients with a history of NPSLE, and we assessed whether apparent diffusion coefficient (ADC) histograms in these patients differ from those of healthy control subjects.**

METHODS: **Eleven female patients with a history of NPSLE (mean age [± SD], 35 years ± 9) and 10 healthy control subjects (eight female, two male; mean age, 37 years ± 16) underwent DWI. DWI and ADC images were assessed by means of visual inspection, and histograms were composed from the ADC images. From these, we derived a variety of parameters that quantitatively reflect the diffusivity of brain parenchyma.**

RESULTS: **Visual inspection of ADC images and DWIs did not reveal any abnormalities in either patients with NPSLE or control subjects. In contrast, ADC histograms of the NPSLE group were, on average, significantly lower and broader, with a higher mean ADC value.**

CONCLUSION: **The data suggest an increased general diffusivity in brain parenchyma of patients with NPSLE, probably based on loss of tissue integrity. In addition to increasing our battery of highly wanted diagnostic tools and our understanding of the pathogenesis of NPSLE, the present method seems to be useful in quantifying the disease burden, enabling monitoring in treatment trials and the study of disease progression.**

In systemic lupus erythematosus (SLE), frequency rates of neurologic, psychiatric, and psychological symptoms as high as 75% have been reported (1, 2). In approximately 40% of patients with SLE, confounding conditions common in SLE patients, such as infections, drug adverse effects, hypertension, and metabolic derangements, can be held responsible for the neuropsychiatric (NP) symptoms (3). The remaining patients with SLE and NP symptoms have what is called neuropsychiatric systemic lupus erythematosus (NPSLE). In patients with NPSLE, clinical signs and symptoms are focal in 25% and diffuse in the remaining. In patients with focal symptoms, neuroimaging modalities often reveal brain infarctions that are attributed to increased coagulability resulting from the presence of antiphospholipid antibodies. In patients with diffuse symptoms, conventional MR images fail to demonstrate abnormalities that provide an explanation for these symptoms (4–7). However, by using advanced techniques such as proton MR spectroscopy (^{1}H–MR spectroscopy), single photon emission CT (SPECT), positron emission tomography (PET), T2 relaxometry, and magnetization transfer imaging (MTI) cerebral abnormalities are found in patients with NPSLE and diffuse symptoms. These are found both during and after episodes with symptoms, and such abnormalities are not observed in SLE patients without NP symptoms (3, 8–10). Still, the nature of the pathophysiologic processes that give rise to diffuse symptoms in patients with NPSLE remains to be elucidated.

Diffusion-weighted imaging (DWI) is another technique that can depict cerebral abnormalities when conventional MR images fail to do so. Qualitative evaluation (clinical reading) of DWIs permits the detection of cytotoxic edema in the early phase of stroke when it is invisible with conventional sequences (11–13). A more quantitative approach comprises the assessment of diffusivity in large volumes of brain tissue, for example, by the generation of apparent diffusion coefficient (ADC) histograms. With this quantitative method, otherwise unapparent differ-

Received June 18, 2002; accepted after revision, December 16.

From the Departments of Radiology (G.P.Th.B., S.P.M., M.A.v.B.) and Rheumatology (T.W.J.H.), Leiden University Medical Center, the Netherlands.

Address reprint requests to G.P.Th. Bosma, MA MD, Department of Radiology C2S, Leiden University Medical Center, PO Box 9600, 2300 RC Leiden, the Netherlands.

TABLE 1: Clinical characteristics, neuropsychiatric symptoms, and radiologic abnormalities of 11 patients with a history of NPSLE

Patient No./ Age/Sex	MR Imaging Abnormalities	Mean WML size, mm	NP Symptoms and Time Since Occurrence*
1/47 y/F	2 WMLs	5 ± 0	Cerebrovascular disease,† 3 mo
2/6 mo/F	Small cerebellar infarction, cerebral atrophy, 2 WMLs	6 ± 1.4	Primary generalized tonic-clonic seizures, 6 mo
3/41 y/F	7 WMLs	3.7 ± 2.0	Movement disorder, 18 mo
4/25 y/F	6 WMLs, cerebral atrophy	3.7 ± 1.0	Absence seizures, 10 mo
5/27 y/F	No WML	NA	Cerebrovascular disease,† 10 mo
6/36 y/F	No WML	NA	Cerebrovascular Disease,† 6 mo
7/49 y/F	21 WML	3.0 ± 1.1	Cranial neuropathy, 2 mo
8/32 y/F	Cerebral trophy, 29 WMLs	6.3 ± 3.9	Cerebrovascular disease,† cognitive dysfunction, 5 mo
9/26 y/F	No WML	NA	Acute confusional state, 10 mo
10/24 y/F	Small venous angioma, left frontal	NA	Absence seizures, 7 mo
11/39 y/F	No WML	NA	Headache from intracranial hypertension, 5 mo

Note.—WML indicates white matter lesion.

* According to the American College of Rheumatology nomenclature and case definitions for NPSLE.

† No infarctions present on MR images obtained at the time of manifestation.

ences are detected between populations (14). We hypothesized that the structural cerebral changes in NPSLE patients with diffuse symptoms might be detectable and quantifiable by means of ADC histogram analysis.

The aim of this preliminary study was to investigate whether the subtle cerebral abnormalities that occur in patients with NPSLE and a history of diffuse symptoms can be detected by using volumetric quantitative DWI analysis.

Methods

Participants

Eleven female patients with NPSLE and a history of diffuse symptoms (mean age [± SD], 35 years ± 9) were age matched with a group of 10 healthy volunteers (eight female, two male; mean age, 37 years ± 16). The patient characteristics, radiologic features, and neuropsychiatric manifestations are listed in Table 1. All patients with SLE fulfilled the 1982 revised criteria of the American College of Rheumatologists (ACR) for SLE (15). The diagnosis of NPSLE was made on clinical grounds and after the exclusion of other causes for neuropsychiatric symptoms, as required by the ACR (16). To eliminate the influence of thromboembolic processes on our results, patients with radiologic evidence of infarctions other than incidental, small (<5 mm), old infarcts were excluded. Patients with NPSLE were not receiving medication for NPSLE, but they might have been taking comedications for concurrent illnesses. All participants provided informed consent, following the guidelines of the independent ethics committee of our institution.

Imaging

MR imaging was performed by using a 1.5-T machine (Philips Medical Systems, Best, the Netherlands). All participants underwent conventional MR imaging, comprising T1-weighted, T2-weighted, proton density–weighted, and fluid-attenuated inversion recovery (FLAIR) imaging, as well as diffusion-weighted echo-planar imaging (EPI) covering the entire brain. DWI consisted of a multishot spin-echo EPI sequence, with an EPI factor defined as the number of Ky profiles collected per excitation of 15; The total TE was 114 ms with a Δ of 47 ms, and the TE was 20 ms. Other parameters were as follows: 256 × 128 matrix, 20 axial sections of 6 mm with an intersection gap of 1 mm, and a field of view of 230 mm covering the whole brain. The b factor was 800 sec/mm^2 applied to measure diffusion in three orthogonal directions. The maximum gradient strength of the machine was 23 mT/m. The slew rate of the system was 105 T/m/sec with a rise time of 0.22 s. The DWI sequence was triggered by the cardiac frequency through a peripheral pulse unit to reduce flow artifacts. Total imaging time was approximately 3 min 28 s, dependent on heart frequency. From the DWI images in each of the three orthogonal directions, an average DWI (DWI_{ave}) was calculated. The diffusion trace, that is, the ADC (ADC_{ave}), was calculated from the DWI_{ave} and b_0 images on a voxel-by-voxel basis. An experienced neuroradiologist (M.A.v.B.) interpreted the conventional images and both the DWI and the ADC image by means of visual inspection.

For postprocessing, the data were exported to a workstation (Ultra 10; Sun Microsystems, Santa Clara, CA). The ADC images were segmented to select the brain parenchyma voxels by using 3DVIEWNIX semi-automated software (Department of Radiology, Hospital of the University of Pennsylvania, Philadelphia). Segmentation consisted of sampling CSF to calculate the mean intensity of CSF in both the DWI_{ave} and b_0 images because, for every individual, a different range of intensity values may occur. Since brain parenchyma always has lower signal intensity values than those of CSF on b_0 images, a threshold was applied to include all voxels with intensity values of 0–80% of the CSF b_0 intensity. To avoid the inclusion of extracranial and background voxels, a threshold was used to include only voxels with intensity values more than 5.5 times the mean intensity of the CSF sample in the DWI_{ave} images. The result of this segmentation on visual inspection was an adequate separation of CSF and brain parenchyma, apart from the exclusion of extracranial structures. At the CSF-parenchymal interface, this method proved to be conservative in that it segmented the brain well within the visible brain boundaries, thereby excluding most voxels that were subjected to partial voluming. In addition, this segmentation process never resulted in the exclusion of voxels within the generated outline of the brain parenchyma. The ADC values of the remaining voxels were subsequently plotted against their matching number in a histogram, as Nusbaum et al recently described (14).

From the ADC histograms, we derived the mean ADC value (ADC_m); the location of the peak (P_{loc}), which was defined as the ADC value corresponding to the largest bin; the SD; a value for kurtosis, which indicated the peakedness of the histogram; a value for skewness, which indicated the shouldering of a histogram (for which a positive value means shouldering to the right and a negative value means shouldering to the left); and the leftsum, which was defined as the area under the curve to the left of the peak. Because the peak height of the histo-

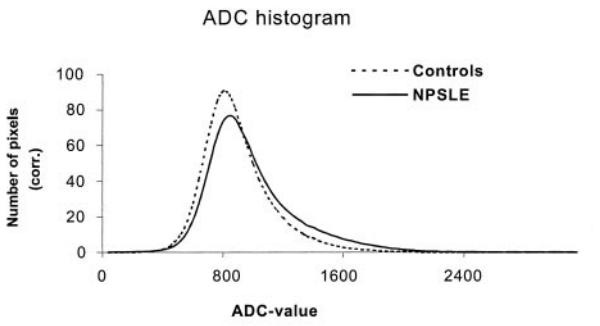

FIG 1. .Mean ADC histograms for patients with a history of NPSLE (*NPSLE*) and the healthy control subjects (*Controls*) corrected for brain size. Note the lower peak height and increased number of pixels with higher ADC values in the NPSLE group.

TABLE 2: Comparison of ADC histogram parameters in patients with a history of NPSLE with healthy control subjects*

Parameter	NPSLE Group (n = 11)	Control Group (n = 10)
H_p	78.0 ± 14.3†	92.7 ± 7.4
P_{loc}	807.3 ± 46.7	776.0 ± 43.0
SD	291.7 ± 43.7†	229.3 ± 31.3
Kurtosis	1.4 ± 0.9	1.6 ± 1.2
Skewness	1.1 ± 0.3	1.0 ± 0.4
ADC_m, × 10^{-6} mm^2/sec	949.4 ± 45.4‡	858.9 ± 37.1
Leftsum	0.40 ± 0.04†	0.45 ± 0.04

* Independent-samples *t* test.
† $P < .01$.
‡ $P < .001$.

gram is influenced by the individual's brain size, the absolute peak was normalized by dividing the number of voxels of the largest bin (the absolute peak) by the total number of brain voxels, that is, the area under the curve. For convenience, this product was multiplied by 1000 to yield a normalized ADC peak height (H_p). Repeat imaging and imaging a third time after repositioning the participants was performed to study the reproducibility of the DWIs and the derived ADC histograms. Both group parameters were compared by using the independent samples *t* test with a *P* value of .01 as level of significance. This way we thought we would minimize the effect of multiple testing.

Results

The abnormalities discovered on visual inspection of the conventional MR images are listed in Table 1. Interpretation of the ADC images and DWIs did not reveal abnormalities that were not observed on images obtained with conventional sequences in either the patients with a history of NPSLE or the control subjects.

The features of the mean ADC histograms of the patients with NPSLE and the control subjects can be seen in Figure 1. The results of a comparison of histogram parameters are displayed in Table 2. The ADC histograms of the healthy control subjects were characterized by a single sharp peak. The size and position of this peak were similar in all healthy subjects, as indicated by both the similar H_p and P_{loc} values and the corresponding low SDs (Fig 1, Table 2). The sharp high peak of the ADC histogram indicated that the brain parenchyma exhibited ADC ratios that were within a narrow range. The other parameters that described the shape of the ADC histograms—H_p, P_{loc}, SD, kurtosis, skewness, ADC_m, and leftsum—were also similar among control subjects. Repeat imaging and imaging a third time after repositioning of these subjects did not significnatly alter the results of the histogram parameters (H_p, P_{loc}, SD, kurtosis, skewness, ADC_m, and leftsum), as can be derived from Figure 2.

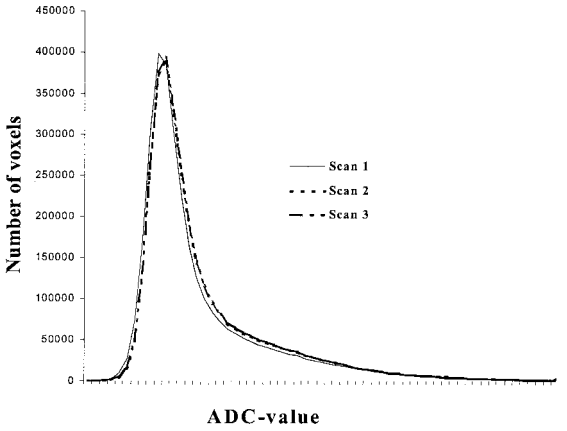

FIG 2. .Uncorrected mean ADC histograms of the 10 control subjects at first-time imaging (*Scan 1*), at repeat imaging (*Scan 2*), and at imaging after repositioning (*Scan 3*). Note the high reproducibility of the ADC histograms.

The shape of the ADC histograms of the NPSLE group was also characterized by a single sharp peak at the same position as that of the control subjects, but the shape of the histograms differed significantly. In the volumetric ADC analysis, the mean H_p value of the NPSLE group was significantly lower ($P < .01$) than the mean H_p value of healthy volunteers. The mean SD and ADC_m values were significantly higher ($P < .01$) in the group of NPSLE patients, compared with the mean values in the group of healthy volunteers. The mean P_{loc} values, as well as mean values for kurtosis, skewness, and leftsum, of both groups did not differ significantly. The lower mean H_p value, in combination with a higher mean SD value and higher mean ADC_m value, indicated that the flatter histograms in the NPSLE group occurred as a result of a preferential increase in the number of voxels with high ADC values. When we excluded the male participants from the healthy volunteers, the same parameters were still significantly different. (for H_p, $P < .01$; for SD, $P < .01$; for kurtosis, $P > .01$; for skewness, $P > .01$; and for ADC_m, $P < .001$). The leftsum value did not meet the strict criteria of a correction for multiple testing, but it was still markedly different ($P < .05$).

Discussion

In the present study, no focal abnormalities of diffusivity were visible on DWIs and ADC images in

patients with a history of NPSLE. Neuronal tracts restrict the movement of free water in one direction without limiting diffusion in the perpendicular direction alongside the tract; this is called anisotropy. Many structures in the brain, such as the thalamus, the optic tract, and the corpus callosum, cause this effect of anisotropy. Interruption of the unidirectional structures decreases anisotropy. Both the DWIs and ADC images used in this study are sensitive to alterations in anisotropy. Still, because no focal or regional lesions were detected by means of diffusion MR imaging, our results suggest either that no structural abnormalities were present in brain parenchyma of patients with a history of NPSLE or that subtle damage was present and did not cause visible abnormalities. To discriminate between both options, quantitative data must be generated, as was done in this study by means of ADC histogram analysis, to compare the included patients with a history of NPSLE with a group of healthy control subjects.

The ADC histogram analysis in the present study revealed abnormal ADC histograms in patients with NPSLE, as indicated by a decreased peak height, an increased SD, and a higher average ADC value, compared with those in the group of control subjects. The flatter and broader histograms in the NPSLE group indicate that, in these patients, widespread increased motility of free-water protons (ie, diffusion) occurs. The subtle white matter hyperintensities that were visible on conventional MR images seemed unlikely to be responsible for the significantly different diffusion pattern in NPSLE because their number and sizes were small. Moreover, these lesions did not appear on DWIs and ADC images; this observation indicates that the diffusivity in the regions with white matter hyperintensities was not markedly altered by their presence. The results of the histogram analysis suggests the option of the presence of subtle and widespread damage in the brain parenchyma of patients with a history of NPSLE. Whether this subtle and widespread damage is confined to certain areas, such as gray matter or white matter, or reflects global cerebral damage should be the subject of forthcoming studies.

The anatomic substrate that causes the deviant diffusion pattern in NPSLE is unknown. In histopathologic studies, demyelination and gliosis have been described in the brain parenchyma of patients with NPSLE (17). Still, the most predominant abnormality described in NPSLE is vasculopathy (1, 18, 19). Vasculopathy might lead to an altered cerebral blood flow, which has been detected by using radionuclide brain scanning, PET, and SPECT in patients with NPSLE (20–27). If hypoperfusion occurs, it might be responsible for the metabolic abnormalities reported in NPSLE patients, as suggested by decreased high-energy phosphate levels in phosporus-31 MR spectroscopic studies and decreased brain oxygen consumption in PET studies (28, 29). The end stage of this process might be axonal loss and associated demyelination, which have been suggested in ^{1}H-MR spectroscopy and MTI studies (9, 10, 30–32).

The results of the current study support the probability of such a pathogenetic pathway. The increased mean ADC value, which was a representative deviant histogram parameter in the NPSLE group, might have been the result of reduced structural integrity (eg, axonal loss and demyelination) in two ways. First, the loss of solid substances permits interstitial water molecules to move in a more unrestricted environment. Second, ADC values decrease by the restriction of motion in a particular direction. The well-organized sheets of myelin form such a boundary. If the structure of these sheets diminishes, ADC values increase. Because the DWI technique used in this study did not provide anisotropy information, our data do not permit an assessment of the precise cause of the observed increased diffusivity. Finally, apart from loss of structural integrity of brain tissue, the observed diffusivity changes could also have been attributed to subtle widening of Virchow-Robin spaces, giving rise to increased subvoxel free-water content.

Still, the exact connection between the reported abnormalities detected with other neuroimaging techniques and the current deviant diffusion patterns is not yet clear. Because the various techniques were applied in different patients, whether the abnormalities reported to date are present in all patients with NPSLE or only in subgroups is impossible to know, given the probability of different pathogeneses. To overcome this problem, studies should be performed in which a combination of these techniques is applied in the same patients. This research might contribute considerably to our knowledge of the pathogenesis of NPSLE and to the development of the best combination of tests to further early diagnosis.

In addition to its contribution to our understanding of the pathogenesis of NPSLE and its probable diagnostic faculties, ADC histogram analysis might also be a useful tool for monitoring the progression of disease in an individual patient. Both the corrected peak height of the ADC histogram and the mean ADC value seem to reflect structural damage, and they might therefore be used as markers of disease burden. A major advantage that seems to make the ADC suitable for both multicenter studies and for monitoring disease progression is its high reproducibility, as indicated by the high similarity between the histogram parameters when the healthy control subjects were imaged three times in this study. Furthermore, ADC values are absolute measures, and for that reason, they might be independent of the techniques used.

Conclusion

In this preliminary study, DWIs and ADC images did not reveal visible abnormalities in brain parenchyma of patients with a history of NPSLE. In contrast, ADC histogram analysis demonstrated increased general diffusivity in these patients, as compared with healthy control subjects. This finding suggests that, in the brain parenchyma of these patients, a loss of tissue integrity occurs and facilitates

motility of free-water protons. In addition to increasing our understanding of the pathogenesis of NPSLE and enlarging our battery of highly wanted diagnostic tools, the present method seems to be useful in quantifying the detected loss of tissue integrity; this ability enables monitoring during treatment trials and the study of disease progression.

Acknowledgments

The authors express their gratitude to Professor P.S. Tofts, Institute of Neurology, University College London, United Kingdom, for critically reading the technical descriptions of this study; to B.C. Stoel, PhD, Division of Image Processing (LKEB) of the Leiden University Medical Center; and to F.G.C. Hoogenraad, PhD, Philips Medical Systems, Best, the Netherlands, for technical support.

References

1. Johnson RT, Richardson EP. **The neurological manifestations of systemic lupus erythematosus.** *Medicine (Baltimore)* 1968;47:337–369
2. Devinsky O, Petito CK, Alonso DR. **Clinical and neuropathological findings in systemic lupus erythematosus: the role of vasculitis, heart emboli, and thrombotic thrombocytopenic purpura.** *Ann Neurol* 1988;23:380–384
3. West SG. **Neuropsychiatric lupus.** *Rheum Dis Clin North Am* 1994; 20:129–158
4. McCune WJ, MacGuire A, Aisen A, Gebarski S. **Identification of brain lesions in neuropsychiatric systemic lupus erythematosus by magnetic resonance scanning.** *Arthritis Rheum* 1988;31:159–166
5. Stimmler MM, Coletti PM, Quismorio FP, Jr. **Magnetic resonance imaging of the brain in neuropsychiatric systemic lupus erythematosus.** *Semin Arthritis Rheum* 1993;22:335–349
6. Gonzalez Crespo MR, Blanco FJ, Ramos A, et al. **Magnetic resonance imaging of the brain in systemic lupus erythematosus.** *Br J Rheumatol* 1995;34:1055–1060
7. Kozora E, West SG, Kotzin BL, Julian L, Porter S, Bigler E. **Magnetic resonance imaging abnormalities and cognitive deficits in systemic lupus erythematosus patients without overt central nervous system disease.** *Arthritis Rheum* 1998;41:41–47
8. Sibbitt W, Sibbitt R, Brooks W. **Neuroimaging in neuropsychiatric systemic lupus erythematosus.** *Arthritis Rheum* 1999;42:2026–2038
9. Bosma GPTh, Rood MJ, Zwinderman AH, Huizinga TWJ, Van Buchem MA. **Evidence of CNS damage in patients with neuropsychiatric systemic lupus erythematosus demonstrated by magnetization transfer imaging.** *Arthritis Rheum* 2000;43:48–54
10. Bosma GPTh, Rood MJ, Huizinga TWJ, De Jong BA, Bollen ELEM, Van Buchem MA. **Detection of cerebral involvement in patients with active neuropsychiatric systemic lupus erythematosus using magnetization transfer imaging.** *Arthritis Rheum* 2000;43: 2428–2436
11. Warach S, Chien D, Li W, Ronthal M, Edelman RR. **Fast magnetic resonance diffusion-weighted imaging of acute human stroke [published erratum appears in Neurology 1992;42:2192].** *Neurology* 1992;42:1717–1723
12. Fisher M, Prichard JW, Warach S. **New magnetic resonance techniques for acute ischemic stroke.** *JAMA* 1995;274:908–911
13. Kucharczyk J, Mintorovitch J, Asgari HS, Moseley M. **Diffusion/perfusion MR imaging of acute cerebral ischemia.** *Magn Reson Med* 1991;19:311–315
14. Nusbaum AO, Tang CY, Wei TC, Buchsbaum MS, Atlas SW. **Whole-brain diffusion MR histograms differ between MS subtypes.** *Neurology* 2000;54:1421–1426
15. Tan EM, Cohen AS, Fries JF, et al. **The 1982 revised criteria for the classification of systemic lupus erythematosus.** *Arthritis Rheum* 1982;25:1271–1277
16. ACR Ad Hoc Committee on Neuropsychiatric Lupus Nomenclature. **The American College of Rheumatology nomenclature and case definitions for neuropsychiatric lupus syndromes.** *Arthritis Rheum* 1999;42:599–608
17. Hanly JG, Walsh NM, Sangalang V. **Brain pathology in systemic lupus erythematosus.** *J Rheumatol* 1992;19:732–741
18. Ellis SG, Verity MA. **Central nervous system involvement in systemic lupus erythematosus: a review of neuropathologic findings in 57 cases, 1955–1977.** *Semin Arthritis Rheum* 1979;8:212–221
19. Zvaifler NJ, Bluestein HG. **The pathogenesis of central nervous system manifestations of systemic lupus erythematosus.** *Arthritis Rheum* 1982;25:862–866
20. Pinching AJ, Travers RL, Hughes GR, Jones T, Moss S. **Oxygen-15 brain scanning for detection of cerebral involvement in systemic lupus erythematosus.** *Lancet* 1978;1:898–900
21. Awada HH, Mamo HL, Luft AG, Ponsin JC, Kahn MF. **Cerebral blood flow in systemic lupus erythematosus with and without central nervous system involvement.** *J Neurol Neurosurg Psychiatry* 1987;50:1597–1601
22. Kushner MJ, Chawluk J, Fazekas F, et al. **Cerebral blood flow in systemic lupus erythematosus with or without cerebral complications.** *Neurology* 1987;37:1596–1598
23. Kovacs JA, Urowitz MB, Gladman DD, Zeman R. **The use of single photon emission computerized tomography in neuropsychiatric SLE: a pilot study.** *J Rheumatol* 1995;22:1247–1253
24. Otte A, Weiner SM, Peter HH, et al. **Brain glucose utilization in systemic lupus erythematosus with neuropsychiatric symptoms: a controlled positron emission tomography study.** *Eur J Nucl Med* 1997;24:787–791
25. Nossent JC, Hovestadt A, Schönfeld DH, Swaak AJ. **Single-photon-emission computed tomography of the brain in the evaluation of cerebral lupus.** *Arthritis Rheum* 1991;34:1397–1403
26. Falcini F, De Cristofaro MT, Ermini M, et al. **Regional cerebral blood flow in juvenile systemic lupus erythematosus: a prospective SPECT study. Single photon emission computed tomography.** *J Rheumatol* 1998;25:583–588
27. Kao CH, Lan JL, ChangLai SP, Liao KK, Yen RF, Chieng PU. **The role of FDG-PET, HMPAO-SPET and MRI in the detection of brain involvement in patients with systemic lupus erythematosus.** *Eur J Nucl Med* 1999;26:129–134
28. Griffey RH, Brown MS, Bankhurst AD, Sibbitt RR, Sibbitt WL, Jr. **Depletion of high-energy phosphates in the central nervous system of patients with systemic lupus erythematosus, as determined by phosphorus-31 nuclear magnetic resonance spectroscopy.** *Arthritis Rheum* 1990;33:827–833
29. Stoppe G, Wildhagen K, Seidel JW, et al. **Positron emission tomography in neuropsychiatric lupus erythematosus.** *Neurology* 1990;40:304–308
30. Davie CA, Feinstein A, Kartsounis LD, et al. **Proton magnetic resonance spectroscopy of systemic lupus erythematosus involving the central nervous system.** *J Neurol* 1995;242:522–528
31. Brooks WM, Sabet A, Sibbitt WL, Jr, et al. **Neurochemistry of brain lesions determined by spectroscopic imaging in systemic lupus erythematosus.** *J Rheumatol* 1997;24:2323–2329
32. Chinn RJ, Wilkinson ID, Hall Craggs MA, et al. **Magnetic resonance imaging of the brain and cerebral proton spectroscopy in patients with systemic lupus erythematosus.** *Arthritis Rheum* 1997; 40:36–46